European Heart Journal – Cardiovascular Imaging (2014) **15**, 85–94
doi:10.1093/ehjci/jet133

Diagnostic performance of hyperaemic myocardial blood flow index obtained by dynamic computed tomography: does it predict functionally significant coronary lesions?

Alexia Rossi[1,2,3], Anoeshka Dharampal[2,3], Andrew Wragg[1], L. Ceri Davies[1], Robert Jan van Geuns[2,3], Costantinos Anagnostopoulos[1], Ernst Klotz[4], Pieter Kitslaar[5,6], Alexander Broersen[6], Anthony Mathur[1], Koen Nieman[2,3], M.G. Myriam Hunink[7,8], Pim J. de Feyter[2,3], Steffen E. Petersen[1†], and Francesca Pugliese[1,9†*]

[1]Centre for Advanced Cardiovascular Imaging, NIHR Cardiovascular Biomedical Research Unit at Barts, William Harvey Research Institute, Barts and The London School of Medicine and Barts Health NHS Trust, The London Chest Hospital, Bonner Road, London E2 9JX, UK; [2]Department of Cardiology, Erasmus MC University Medical Centre Rotterdam, Rotterdam, The Netherlands; [3]Department of Radiology, Erasmus MC University Medical Centre Rotterdam, Rotterdam, The Netherlands; [4]Siemens Healthcare Sector, Forchheim, Germany; [5]Medis Medical Imaging Systems, Leiden, The Netherlands; [6]Division of Image Processing, Department of Radiology, Leiden University Medical Center, Leiden, The Netherlands; [7]Department of Clinical Epidemiology, Erasmus MC University Medical Centre Rotterdam, Rotterdam, The Netherlands; [8]Harvard School of Public Health, Boston, MA, USA; and [9]Department of Cardiology, Arhus University Hospital, Arhus, Denmark

Received 14 May 2013; accepted after revision 21 June 2013; online publish-ahead-of-print 9 August 2013

Aims The severity of coronary artery narrowing is a poor predictor of functional significance, in particular in intermediate coronary lesions (30–70% diameter narrowing). The aim of this work was to compare the performance of a quantitative hyperaemic myocardial blood flow (MBF) index derived from adenosine dynamic computed tomography perfusion (CTP) imaging with that of visual CT coronary angiography (CTCA) and semi-automatic quantitative CT (QCT) in the detection of functionally significant coronary lesions in patients with stable chest pain.

Methods and results CTCA and CTP were performed in 80 patients (210 analysable coronary vessels) referred to invasive coronary angiography (ICA). The MBF index (mL/100 mL/min) was computed using a model-based parametric deconvolution method. The diagnostic performance of the MBF index in detecting functionally significant coronary lesions was compared with visual CTCA and QCT. Coronary lesions with invasive fractional flow reserve of $\leq$0.75 were defined as functionally significant. The optimal cut-off value of the MBF index to detect functionally significant coronary lesions was 78 mL/100 mL/min. On a vessel-territory level, the MBF index had a larger area under the curve (0.95; 95% confidence interval [95% CI]: 0.92–0.98) compared with visual CTCA (0.85; 95% CI: 0.79–0.91) and QCT (0.89; 95% CI: 0.84–0.93) (both *P*-values $<$0.001). In the analysis restricted to intermediate coronary lesions, the specificity of visual CTCA (69%) and QCT (77%) could be improved by the subsequent use of the MBF index (89%).

Conclusion In this proof-of-principle study, the MBF index performed better than visual CTCA and QCT in the identification of functionally significant coronary lesions. The MBF index had additional value beyond CTCA anatomy in intermediate coronary lesions. This may have a potential to support patient management.

Keywords coronary artery disease • myocardial blood flow • myocardial perfusion • coronary computed tomography angiography • dynamic contrast-enhanced computed tomography

† F.P. and S.E.P. contributed equally to this work and as joint last authors.

* Corresponding author. Tel: +44 20 7882 6906, Email: f.pugliese@qmul.ac.uk

Introduction

Computed tomography coronary angiography (CTCA) is an established non-invasive imaging modality for the diagnosis of coronary artery disease. Similar to invasive coronary angiography (ICA), CTCA evaluates the anatomical severity of coronary lesions. Anatomical CTCA findings are poor predictors of functionally significant coronary lesions, in particular in lesions of intermediate severity (30–70% diameter reduction). Additional functional testing is often required to guide patient management. Fractional flow reserve (FFR) is commonly used during ICA for the identification of functionally significant coronary lesions to guide angioplasty.[1] Stress dynamic CT perfusion (CTP) imaging is a newly introduced non-invasive technique that allows the absolute quantification of a myocardial blood flow (MBF) index. Combined with CTCA, this MBF index may allow a more comprehensive non-invasive evaluation of patients with suspected coronary artery disease. To date, only few animal studies[2–6] and small single-centre patient series[7–10] have shown the feasibility of this method. The purpose of this prospective study was to evaluate the diagnostic performance of such MBF index obtained by dynamic CTP imaging during hyperaemic stress for the identification of functionally significant coronary lesions in patients with stable angina. We hypothesized that the MBF index would have a better diagnostic performance than anatomical CTCA, in particular in coronary lesions of intermediate severity.

Methods

Study population

From March 2011 to September 2012, 157 patients with stable chest pain scheduled for ICA at two large institutions were screened for inclusion into this prospective study (*Figure 1*). Patients underwent a CT study consisting of CTCA and adenosine stress dynamic CTP 1 day to 2 weeks before ICA. Exclusion criteria were acute coronary syndrome, severely impaired left ventricular ejection fraction (≤35%), estimated glomerular filtration rate (eGFR) <60 mL/min, documented or suspected allergy to iodinated contrast and contraindications to adenosine infusion such as history of severe asthma or obstructive lung disease, second- or third-degree atrioventricular block, and a systolic blood pressure <90 mmHg. The study protocol was compliant with the declaration of Helsinki and received approval by the Research Ethics Committee/Institutional Review Board at each institution. All patients gave written informed consent.

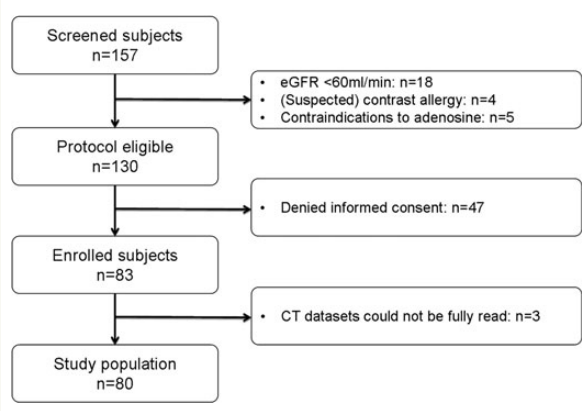

Figure 1 Inclusion procedure.

CT protocol

A second-generation dual-source CT scanner (Somatom Definition Flash, Siemens, Forchheim, Germany) was used at both institutions. The preparation procedure and scan protocol for CTCA and stress dynamic CTP are detailed in Appendix 1. The median (interquartile range, IQR) dose-length product (DLP) associated with CTCA was 302 (215–402) Gy cm (using a conversion factor for the chest of 0.014 this corresponds to 4.2 mSv). The median (IQR) DLP for CTP was 674 (621–748) Gy cm (9.4 mSv). A total volume of 115–135 mL of contrast agent was used for the whole CTCA/CTP protocol.

CTCA and CTP analysis

A flow-chart of CT image analysis is given in Appendix 2. Anonymized CTCA data were analysed blindly in a core-lab based at Erasmus MC, Rotterdam. An off-line workstation with a commercially available platform (syngo 3D, MMW, Siemens, Erlangen, Germany) was used. If more than one lesion was present within the same vessel, the most severe lesion was selected and used in the analysis. Lesion severity was assessed visually, and then quantified using semi-automatic software (QAngioCT Research Edition v1.3.61, Medis Medical Imaging Systems, Leiden, the Netherlands). For the latter, percentage diameter narrowing was calculated from detected lumen contours at the minimal lumen area and corresponding reference diameter values obtained from an automatic trend analysis of the vessel area.[11] The percent diameter narrowing assessed visually and measured by quantitative CT (QCT) was dichotomized using three thresholds: (i) ≥30% vs. <30%, (ii) ≥50% vs. <50%, and (iii) ≥70% vs. <70% diameter narrowing.

Anonymized stress CTP images were analysed blindly at a core-lab based at the Centre for Advanced Cardiovascular Imaging, London. Commercial software (Volume Perfusion CT Body, Siemens)[4] was used (Appendix 2). The MBF index in each voxel was calculated as the maximum slope of the fit curve/maximum arterial input function, and quantitative three-dimensional colour maps representing MBF index distribution in the myocardium were created. Three 10-mm thick standard short-axis views of the left ventricle at basal, mid-cavity, and apical levels were generated. Measurements of MBF index were obtained from regions of interest of at least 1000 pixels (i.e. at least 0.5 cm^2) positioned in a representative area of each myocardial segment according to a standard 16-segment model.[12] Individual myocardial segments supplied by the same coronary vessel based on a three-vessel-territory model [left anterior descending coronary artery (LAD), left circumflex coronary artery, and right coronary artery (RCA)] were considered as parts of the same territory. Within each territory, the myocardial segment with the lowest MBF index was selected and used in the analysis. To ensure accurate matching of coronary vessels and associated myocardial territories, coronary dominance (right, left, or balanced) was used to decide which vessel (RCA, left coronary artery, or both) supplied the inferior and infero-septal segments of the myocardium. The time needed to post-process and analyse a CT perfusion dataset was ~8 min.

ICA and FFR

All patients underwent ICA. During the procedure, two experienced interventional cardiologists visually identified coronary lesions associated with diameter narrowing between 30 and 90%. FFR was measured using a sensor-tipped 0.014-inch guidewire (Pressure Wire, Radi Medical Systems, Uppsala, Sweden). The pressure sensor was positioned just distal to the lesion, and maximal myocardial hyperaemia was induced

by a continuous intravenous infusion of adenosine in a femoral vein (140 μg/kg/min for a minimum of 2 min). The FFR was calculated as the ratio of mean distal pressure measured by the pressure wire divided by the mean proximal pressure measured by the guiding catheter. ICA images were analysed blindly on multiple projections by a single experienced observer unaware of the CT results. The most severely diseased segment in each coronary vessel was identified to derive percentage diameter narrowing using validated quantitative coronary angiography (QCA) software (QAngio® XA, 7.2, Medis, Leiden, the Netherlands).

Standard of reference

If FFR was ≤0.75 lesions were classified as functionally significant; if FFR was >0.75 lesions were classified as non-significant. Critical lesions (≥90% diameter narrowing) were classified as significant, while mild lesions (<30% diameter narrowing) were classified as non-significant.[13]

Statistical analysis

Statistical analysis was performed using commercial software (IBM SPSS Statistic, version 20; Somers, NY, USA). Results were reported in accordance with the STARD criteria.[14] Continuous variables were presented as means ± standard deviations (SD) or medians with interquartile ranges (IQRs). Categorical variables were presented as frequencies and percentages. Intra- and inter-observer variability were calculated using intraclass correlation coefficients (ICC's). The time interval between repeat readings by the same observer was >3 months. Receiver operating characteristic (ROC) curves were built for MBF index, CTCA, and QCT. The optimal cut-off value of the MBF index was identified as the value that allowed the optimization of specificity, provided that sensitivity was at least 85%. For the purpose of this analysis, myocardial territories downstream to non-significant coronary lesions were defined as remote myocardium. MBF index values in territories downstream to significant lesions were compared with the remote myocardium using the Wilcoxon signed-rank test. Sensitivity analyses used the specified cut-off value of MBF index. At the patient level, sensitivity and specificity were calculated as proportions with 95% confidence intervals. The vessels with the most severe findings were selected to represent the patient (lowest FFR and lowest MBF index). At the vessel-territory level, we adjusted for the clustered nature of the data using logistic generalized estimating equations (GEE's).[15] Secondly, we performed a pre-specified sub-analysis in vessels directly interrogated with FFR. Thirdly, we estimated the diagnostic performance in intermediate coronary lesions defined as diameter narrowing between 30 and 70% on CTCA. The DeLong test was used to compare the areas under the curve (AUC's) of MBF index with those of visual CTCA and QCT. The McNemar test was used to compare sensitivity and specificity. Univariable GEE models were used to assess the value of CTCA and QCT in predicting functional significance in intermediate coronary lesions. The incremental value of the MBF index over CTCA and QCT was evaluated comparing the AUC's of the multivariable models with that of the corresponding univariable models.

Results

Baseline characteristics and ICA findings

The study population consisted of 80 patients (*Figure 1*). Stents were present in 13 vessels, and these were excluded from analysis. Further three vessels were excluded due to suboptimal ICA views. One vessel could not be engaged on ICA due to an anomalous origin. Further 11 vessels and 2 myocardial territories were excluded due to poor image quality on CTCA and CTP, respectively. Thus, data from 210 coronary vessels and 210 corresponding myocardial territories were available for comparison and were included in the analysis.

Functionally significant coronary lesions were found in 56 of 210 (27%) vessels in 40 of 80 (50%) patients. There were 3 of 80 patients with three-vessel disease, 10 with two-vessel disease, and 27 with one-vessel disease. Baseline characteristics of the population are given in *Table 1*. The FFR was measured in 68 vessels and ranged between 0.24 and 1.00 (median 0.79; IQR: 0.71–0.87). An FFR of ≤0.75 was found in 25 of 68 (37%) vessels.

Table 1 Baseline characteristics and main ICA findings (*N* = 80)

Characteristics	Total (*N* = 80)
Men/women	63/17 (79%/21%)
Age (years)	60 ± 10
Body mass index (kg/m^2)	27 ± 4
Risk factors	
Diabetes mellitus[a]	16 (20%)
Hypertension[b]	48 (60%)
Dyslipidaemia[c]	53 (66%)
Current smoker	26 (33%)
Family history of coronary artery disease[d]	35 (44%)
Agatston calcium score: median (IQR)	198 (26–618)
Right dominant coronary system	72 (90%)
Heart rate (bpm)	
Baseline	66 ± 11
During hyperaemia	87 ± 14
Systolic blood pressure (mmHg)	
Baseline	135 ± 23
During hyperaemia	128 ± 21
Diastolic blood pressure (mmHg)	
Baseline	76 ± 11
During hyperaemia	70 ± 13
Patients with functionally significant coronary lesion[e]	40/80 (50%)
One-vessel disease	27/80 (34%)
Two-vessel disease	10/80 (12%)
Three-vessel disease	3/80 (4%)
Vessels with functionally significant coronary lesion[e]	56/210 (27%)
Right coronary artery	14/56 (25%)
Left main/left anterior descending coronary artery[f]	28/56 (50%)
Left circumflex artery	14/56 (25%)

Values are means ± SD, or frequencies (percentages), unless otherwise specified.
[a]Treatment with oral anti-diabetic medication or insulin.
[b]Blood pressure of ≥140/90 mmHg or treatment for hypertension.
[c]Total cholesterol of >180 mg/dL or treatment for hypercholesterolaemia.
[d]Family history of coronary artery disease having first- or second- degree relatives with premature coronary artery disease (age <55 years).
[e]Functionally significant coronary lesion defined as FFR of ≤0.75 or QCA diameter narrowing of ≥90%.
[f]Only one patient had significant left main disease associated with significant disease of the left anterior descending and left circumflex arteries.

CTP and MBF index

CTP was performed 7 ± 5 days before ICA (range 1–14 days). No severe adverse reactions to adenosine or contrast were observed. The median (IQR) MBF index in the whole sample was 97 (74–127) mL/100 mL/min. The median MBF index was 62 (51–74) mL/100 mL/min in myocardial territories downstream to vessels with functionally significant coronary lesions and 109 (92–136) mL/100 mL/min in the remote myocardium ($P < 0.001$). The median MBF index was: a) 57 (50–68) mL/100 mL/min in myocardial territories downstream to ≥90% coronary diameter narrowing; b) 70 (62–75) mL/100 mL/min downstream to 30–89% coronary diameter narrowing and FFR ≤0.75; c) 98 (82–115) mL/100 mL/min downstream to 30–89% coronary diameter narrowing and FFR >0.75; d) 114 (94–138) mL/100 mL/min downstream to <30% coronary diameter narrowing. The MBF index in vessels directly interrogated with FFR is shown in *Figure 2*. Intra- and inter-observer ICC's were 0.86 (95% CI: 0.78–0.91) and 0.82 (95% CI: 0.73–0.88), respectively.

Diagnostic performance in the whole sample (total vessels = 210)

On a vessel-territory level, MBF index had an AUC of 0.95 (95% CI: 0.92–0.98, $P < 0.001$). All territories with an MBF index of <51 mL/100 mL/min were downstream to functionally significant lesions. All territories with an MBF index of >103 mL/100 mL/min were supplied by non-obstructive vessels (remote myocardium). An MBF index cut-off value of 78 mL/100 mL/min yielded 88% sensitivity and 90% specificity (*Figure 3A*). Visual CTCA had an AUC of 0.85 (95% CI: 0.79–0.91, $P < 0.001$), and QCT had an AUC of 0.89 (95% CI: 0.84–0.93, $P < 0.001$). The diagnostic performance of MBF index was better than that of visual CTCA ($P < 0.001$) and QCT ($P = 0.014$). QCT performed slightly better than visual CTCA ($P = 0.019$) (*Figure 3B*). Sensitivity, specificity, positive predictive value (PPV), and negative predictive value (NPV) of MBF index, CTCA, and QCT are given in *Table 2*.

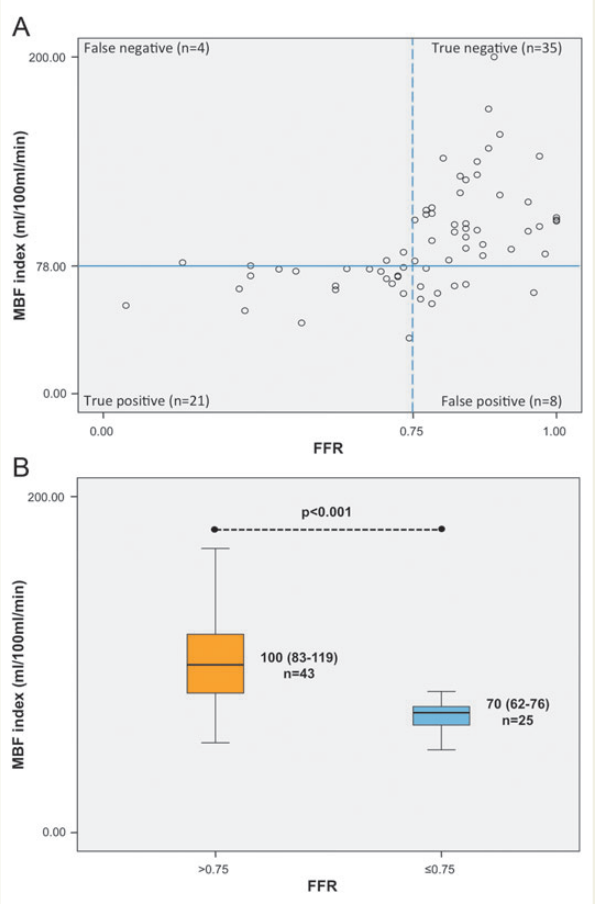

Figure 2 Hyperaemic MBF index in vessels interrogated with FFR ($n = 68$). (*A*) Scatter plot shows MBF index in a given myocardial territory and FFR in the corresponding vessel. (*B*) Hyperaemic MBF index was lower in vessels with FFR of ≤0.75 compared with that in vessels with FFR >0.75 (MBF index values are medians and interquartile ranges).

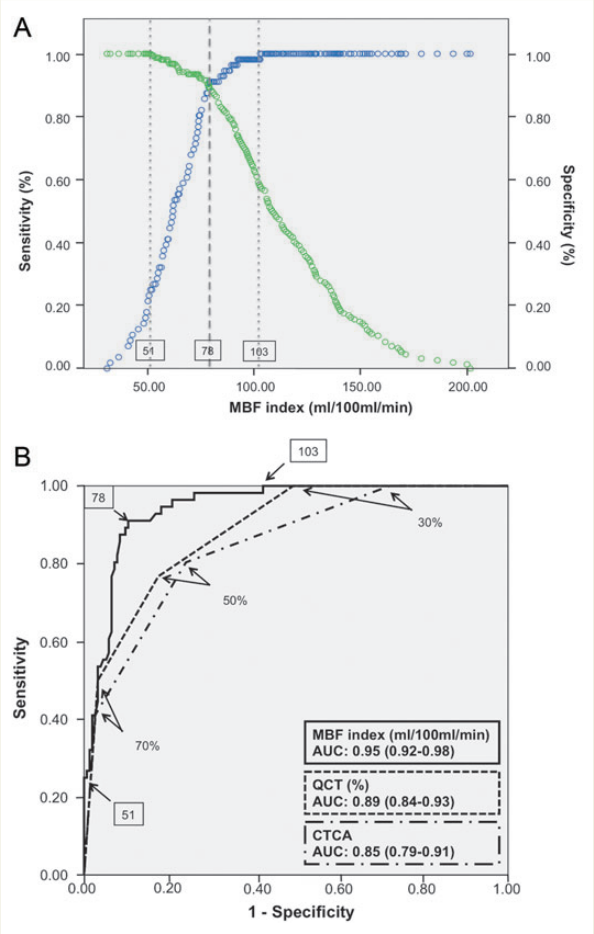

Figure 3 Diagnosis of functionally significant coronary lesion (vessel-territory level). (*A*) A cut-off value for MBF index of 78 mL/100 mL/min yielded 88% sensitivity and 90% specificity. (*B*) ROC curves showed a better performance for MBF index compared with visual CTCA and QCT ($P < 0.001$ and 0.014, respectively). QCT performed better than visual CTCA ($P = 0.019$).

Table 2 Diagnostic performance of visual CTCA, QCT, and MBF index

	TP	TN	FP	FN	Sensitivity, % (95% CI)	Specificity, % (95% CI)	PPV, % (95% CI)	NPV, % (95% CI)
Functionally significant coronary lesion as the standard of reference								
Vessel-territory level ($N = 210$)								
Visual CTCA—30%	56	43	111	0	100 (94–100)	28 (21–36)[§]	34 (27–41)	100 (92–100)
Visual CTCA—50%	45	117	37	11	80 (67–89)	76 (67–83)[§]	55 (43–66)	91 (85–95)
Visual CTCA—70%	24	150	4	32	43 (31–55)[∫]	97 (93–99)	86 (67–95)	82 (76–87)
QCT—30%	56	76	74	0	100 (94–100)	51 (41–60)[§]	42 (34–51)	100 (95–100)
QCT—50%	43	127	27	13	77 (63–87)	83 (75–88)	61 (49–72)	91 (85–95)
QCT—70%	28	149	5	28	50 (37–63)[∫]	97 (91–99)	85 (66–94)	84 (78–89)
MBF index	49	139	15	7	88 (74–95)[a]	90 (82–95)[a]	77 (61–87)[a]	95 (90–98)[a]
Patient level ($N = 80$)								
Visual CTCA—30%	40	7	33	0	100 (91–100)	18 (9–32)[§]	55 (43–66)	100 (65–100)
Visual CTCA—50%	33	25	15	7	83 (69–91)	63 (47–76)[§]	69 (55–80)	78 (61–89)
Visual CTCA—70%	21	37	3	19	53 (38–67)[∫]	93 (87–97)	88 (69–96)	66 (53–77)
QCT—30%	40	16	24	0	100 (91–100)	40 (26–55)	63 (50–73)	100 (81–100)
QCT—50%	31	29	11	9	78 (63–88)	73 (57–84)[§]	74 (59–85)	76 (61–87)
QCT—70%	24	37	3	16	60 (45–74)[∫]	93 (80–97)	89 (72–96)	70 (57–81)
MBF index	36	35	5	4	90 (77–96)[a]	88 (74–94)[a]	88 (75–95)[a]	90 (76–96)[a]
Sub-analysis including vessels directly interrogated with FFR								
Vessel-territory level ($N = 68$)								
Visual CTCA—30%	25	3	40	0	100 (87–100)	7 (2–19)[§]	39 (28–51)	100 (44–100)
Visual CTCA—50%	18	24	19	7	72 (50–87)	56 (38–72)[§]	49 (32–65)	77 (58–90)
Visual CTCA—70%	9	40	3	16	36 (18–59)[∫]	93 (81–98)	75 (43–92)	71 (58–82)
QCT—30%	25	11	32	0	100 (87–100)	26 (13–45)[§]	44 (31–58)	100 (74–100)
QCT—50%	16	32	11	9	64 (42–81)	74 (59–86)	59 (40–76)	78 (62–88)
QCT—70%	9	42	1	16	36 (20–57)[∫]	98 (85–100)	90 (53–99)	72 (59–83)
MBF index	21	35	8	4	84 (64–94)[a]	81 (64–92)[a]	72 (53–86)[a]	90 (77–96)[a]

CTCA—30%, visual analysis with ≥30% diameter narrowing to define positive cases; CTCA—50%, visual analysis with ≥50% diameter narrowing to define positive cases; CTCA—70%, visual analysis with ≥70% diameter narrowing to define positive cases; QCT—30%, semi-automatic quantitative CTCA analysis with ≥30% diameter narrowing to define positive cases; QCT—50%, semi-automatic quantitative CTCA analysis with ≥50% diameter narrowing to define positive cases; QCT—70%, semi-automatic quantitative CTCA analysis with ≥70% diameter narrowing to define positive cases; CI, confidence interval; TP, true positive; TN, true negative; FP, false positive; FN, false negative; PPV, positive predictive value; NPV, negative predictive value.

[a]MBF index cut-off value: 78 mL/100 mL/min.

[∫]$P < 0.05$; sensitivity significantly lower than MBF's sensitivity using the McNemar test.

[§]$P < 0.05$; specificity significantly lower than MBF's specificity using the McNemar test.

Diagnostic performance in vessels directly interrogated with FFR (vessels = 68)

MBF index had an AUC of 0.85 (95% CI: 0.76–0.94, $P < 0.001$), 84% sensitivity and 81% specificity. PPV and NPV were 72% and 90%, respectively. Visual CTCA had an AUC of 0.69 (95% CI: 0.56–0.83, $P < 0.001$), and QCT had an AUC of 0.78 (95% CI: 0.66–0.89, $P < 0.001$). The diagnostic performance of the MBF index was better than visual CTCA and QCT (both *P*-values <0.001). QCT performed slightly better than visual CTCA ($P < 0.001$) (*Table 2*).

Diagnostic performance in intermediate coronary lesions on CTCA (30–70% diameter reduction)

In the analysis restricted to coronary lesions scored between 30 and 70% diameter reduction on CTCA, on a vessel-territory level, MBF index had an AUC of 0.87 (95% CI: 0.79–0.95, $P < 0.001$), 85% sensitivity and 89% specificity. PPV and NPV were 70% and 95%, respectively. Visual CTCA had an AUC of 0.68 (95% CI: 0.57–0.79, $P = 0.002$), and QCT had an AUC of 0.69 (95% CI: 0.58–0.80, $P = 0.001$). The diagnostic performance of the MBF index was better than visual CTCA ($P = 0.003$) and QCT ($P = 0.002$) due to a significantly lower false positive ratio (better specificity) (*Table 3*).

Incremental value of the MBF index over CTCA and QCT

Coronary diameter narrowing of ≥50 and ≥70% on CTCA and QCT were independent predictors of functionally significant lesions. When MBF index was added to CTCA and to QCT in a multivariable model, a significant increase in the model's AUC confirmed that MBF index had incremental value over CTCA (AUC's 0.94 vs. 0.78) and QCT (AUC's 0.94 vs. 0.79). In coronary lesions between

Table 3 Diagnostic performance of visual CTCA, QCT, and MBF index (vessel-territory level) for lesions of intermediate severity (30–70% diameter narrowing on visual CTCA) in 69 patients

	TP	TN	FP	FN	Sensitivity, % (95% CI)	Specificity, % (95% CI)	PPV, % (95% CI)	NPV, % (95% CI)
Functionally significant coronary lesion as standard of reference ($N = 140$)								
Visual CTCA—50%	22	74	33	11	67 (47–82)	69 (58–78)[∫]	40 (27–57)	87 (78–93)
QCT—50%	20	82	25	13	61 (42–77)	77 (67–84)[∫]	44 (31–59)	86 (78–92)
MBF index	28	95	12	5	85 (69–94)[a]	89 (78–95)[a]	70 (50–85)[a]	95 (89–98)[a]
Sub-analysis including vessels directly interrogated with FFR ($N = 54$)								
Visual CTCA—50%	10	21	16	7	59 (33–81)	57 (38–74)[∫]	39 (21–60)	75 (54–87)
QCT—50%	8	27	10	9	47 (24–72)	73 (56–85)	44 (22–69)	75 (58–87)
MBF index	13	31	6	4	77 (53–91)[a]	84 (64–94)[a]	68 (40–88)[a]	89 (75–95)[a]

All other abbreviations as in *Table 2*.
[∫] $P < 0.05$; specificity significantly lower than MBF's specificity using the McNemar test.

30 and 70% diameter reduction, MBF index maintained its incremental value over CTCA (AUC's 0.92 vs. 0.68) and QCT (AUC's 0.90 vs. 0.69) (*Table 4*).

Discussion

Summary of main findings

In this study, we evaluated the diagnostic performance of hyperaemic MBF index derived from stress dynamic CTP imaging to identify functionally significant coronary lesions in comparison with visual CTCA and QCT. All patients underwent ICA with FFR independently of the CT results. We used stringent positivity criteria based on FFR and ICA to define functionally significant coronary lesions as the study endpoint. Myocardial territories supplied by functionally significant coronary lesions could be differentiated reliably from the remote myocardium. The performance of MBF index (AUC: 0.95) was better than that of CTCA and QCT (AUC's: 0.85 and 0.89, respectively), both on a vessel-territory level as well as on a patient-level. In the sub-analysis restricted to lesions scored as intermediate on CTCA (30–70% diameter narrowing), the performance of the MBF index (AUC: 0.87) remained better than CTCA or QCT (AUC's: 0.68 and 0.69, respectively).

MBF index

Our study used a dynamic CTP technique that is fundamentally different from static techniques. Unlike static perfusion, where a single set of images is acquired at a single time point within the early arterial phase,[16–21] dynamic CTP imaging involves repeated imaging over time to capture the inflow and washout of contrast in the myocardial tissue and vascular compartment to construct time-attenuation curves (TAC's) from which a quantitative MBF index can be computed.[4] In contrast to static CTP, such quantitative MBF index does not rely on the assumption that the best-enhanced territory is normal and can be used as reference. The MBF index provides independent information about each myocardial territory. Quantification of images in general results in more precise and reproducible findings. A quantitative MBF index might be particularly useful in cases where relative assessment of lesions' functional significance is difficult such as patients with balanced multivessel disease.[22,23] For these reasons, we chose not to rely on a visual approach to detect differences in myocardial enhancement. In our study, the absolute value of MBF index to discriminate functionally significant coronary lesions from non-flow-limiting lesions was 78 mL/100 mL/min. This is in keeping with the value of 75 mL/100 mL/min found by Bamberg *et al.*[7] Using this cut-off, we could identify all functionally significant coronary lesions in patients with three-vessel disease (*Figure 4*). It is noteworthy that we could not distinguish whether a hyperaemia-induced CTP abnormality was reversible or irreversible (myocardial scar) since this would have required further CTP scan at rest. However, FFR was our reference standard and a decrease in FFR in a lesion supplying an area of myocardial scar cannot be expected.[24] Thus, in this proof-of-principle study, we decided to restrict the associated radiation exposure and volume of contrast agent. Accordingly, we excluded from analysis the myocardial territories downstream to coronary vessels with previously implanted stents. The normal values of MBF in healthy subjects during hyperaemia are in the range of 200–500 mL/100 g/min.[25] The MBF index values found in this study were lower. MBF measured by different imaging modalities (positron emission tomography, magnetic resonance imaging, single-photon emission tomography, and CT) may differ due to different uptake kinetics of the tracers or contrast agents used, different acquisition protocols, and post-processing methods.[10,23,26] In our analysis, we did not average values of MBF index, but selected the lowest MBF index measurement in each vascular territory as the most representative ischaemic area in that territory. Difficulty in temporal sampling of the hyperaemic intra-capillary first pass of contrast, which is characterized by fast flow, may be a further explanation for this difference.

Diagnostic performance

Anatomical diameter narrowing is a poor indicator of flow-limiting lesion even by ICA.[13] In this study, the MBF index

Table 4 Incremental value of MBF index

	DOR (95% CI)	*P*-values	AUC (95% CI)
All patients ($N = 80$), vessel-territory level ($N = 210$)			
Univariable GEE			
Visual CTCA—50%	12 .9 (6.1–27.5)	<0.001	0.78 (0.71–0.85)
Visual CTCA—70%	28.1 (9.1–86.6)	<0.001	0.70 (0.61–0.79)
QCT—50%	15.6 (7.4–32.8)	<0.001	0.79 (0.72–0.87)
QCT—70%	29.8 (10.6–83.8)	<0.001	0.73 (0.65–0.82)
Multivariable GEE			
Model 1			
Visual CTCA—50%	7.4 (2.7–20.1)	<0.001	0.94 (0.91–0.97)
MBF index	45.8 (16.6–126.0)	<0.001	
Model 2			
Visual CTCA—70%	14.7 (3.2–67.6)	0.001	0.92 (0.87–0.97)
MBF index	49.3 (17.8–136.3)	<0.001	
Model 3			
QCT—50%	8.9 (3.2–24.3)	<0.001	0.94 (0.90–0.98)
MBF index	44.5 (15.9–124.8)	<0.001	
Model 4			
QCT—70%	30.0 (6.6–133.0)	<0.001	0.93 (0.89–0.98)
MBF index	64.7 (20.3–205.5)	<0.001	
Patients with intermediate coronary lesions ($N = 69$), vessel-territory level ($N = 140$)			
Univariable GEE			
Visual CTCA—50%	4.49 (1.88–10.73)	0.001	0.68 (0.57–0.79)
QCT—50%	5.05 (2.19–11.64)	<0.001	0.69 (0.58–0.80)
Multivariable GEE			
Model 1			
Visual CTCA—50%	3.17 (0.84–11.97)	0.088	0.92 (0.87–0.94)
MBF index	38.76 (11.15–134.79)	<0.001	
Model 2			
QCT—50%	3.07 (0.88–10.73)	0.079	0.90 (0.84–0.97)
MBF index	36.92 (10.69–127.54)	<0.001	

All other abbreviations as in *Table 2*.
Univariable and multivariable GEE models for the prediction of functionally significant coronary lesions.
MBF index cut-off value: 78 mL/100 mL/min.
GEE, generalized estimating equation; DOR, diagnostic odds ratio; AUC, area under the curve; CI, confidence interval.

performed well in the identification of functionally significant lesions compared with FFR, showing that non-invasive imaging has a potential value to combine functional information with anatomy as guidance to revascularization procedures.[1] MBF index had better discriminatory power than visual CTCA and QCT to identify and exclude flow-limiting lesions, both on a patient-level and on a vessel-territory level. The performance of a semi-automatic quantitative method (QCT) to measure coronary artery narrowing was better than visual CTCA but inferior to the MBF index. MBF index had 90% sensitivity and 88% specificity in the identification of patients with functionally significant lesions, which compared well with other imaging modalities, either qualitative or quantitative. For instance, qualitative single-photon emission tomography had 85% sensitivity and 85% specificity.[27] Quantitative positron emission tomography had 95% sensitivity and 91% specificity,[28] and quantitative magnetic resonance imaging had 82% sensitivity and 81% specificity.[26]

Clinical implications: incremental value in intermediate coronary lesions

Intermediate coronary lesions (30–70% diameter narrowing) represent a challenge as their functional significance is hard to predict. Anatomical CTCA yielded both false positive and false negative findings in these lesions, in keeping with previous reports.[29,30] Since revascularization of a coronary lesion is only justified if the lesion is functionally significant,[31] we sought to evaluate whether there was an additional value of the MBF index over visual CTCA or QCT in intermediate coronary lesions. We followed an approach consisting of anatomical testing first (CTCA) to identify intermediate coronary lesions followed by functional testing (MBF index) (*Table 3*). Such an approach was different from that followed by Bamberg *et al.*,[7] where only lesions with ≥50% diameter narrowing on CTCA were reclassified based on the MBF index. By the identification of intermediate coronary lesions first, as it can be obtained from modern

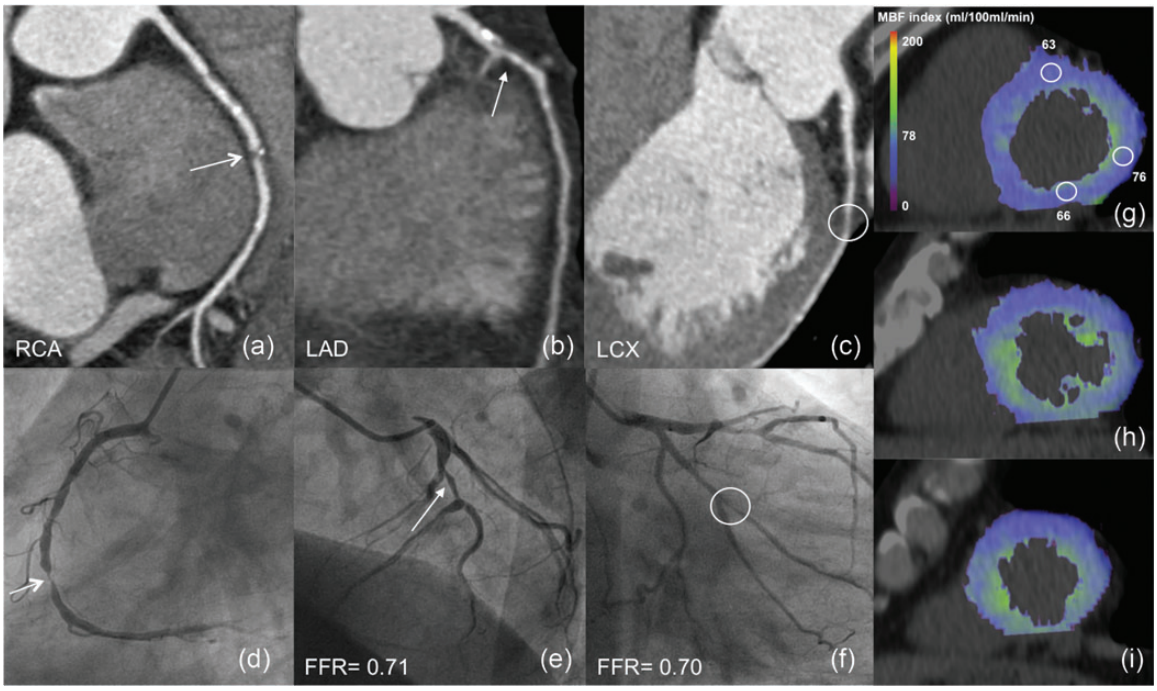

Figure 4 Stress dynamic CTP imaging in a patient with three-vessel disease. Sixty-year-old man with stable chest pain, hypertension, and family history of coronary artery disease. (*A*–*C*) CTCA showed severe coronary lesion (>70% narrowing) in the mid right coronary artery (RCA) (arrow; A) and moderate lesions (50–69% narrowing) in the mid left anterior descending coronary artery (LAD) (arrow; B), and in the obtuse marginal branch (circle; C). ICA confirmed the critical lesion in the mid-RCA (*D*). Both the LAD and obtuse marginal lesions were functionally significant at FFR (*E* and *F*). Colour-coded stress dynamic CTP maps in basal (*G*), mid (*H*), and apical (*I*) short-axis views demonstrated a reduced MBF index (<78 mL/100 mL/min) in the whole myocardium.

CTCA with low radiation exposure to the patient, we observed a significant gain in discriminatory power of MBF index compared with CTCA and QCT with a significant reduction in false positive findings. MBF index had an incremental value over ≥50% diameter narrowing on CTCA and QCT (*Table 4*). In this context, the possibility of non-invasive FFR,[32] albeit still computationally difficult, may further enhance the clinical value of CT in patients with coronary artery disease.

Limitations

Our study was performed in stable patients referred to ICA who consented to participate in this study. Vessels and myocardial territories with poor CT image quality were excluded, as were patients with acute coronary syndromes. Among patients with demonstrated significant coronary artery lesions, the majority had one-vessel disease. This study should be considered a proof-of-principle study and it remains to be demonstrated whether a similar high diagnostic performance can be achieved in less-selected populations. Invasive FFR, considered a reliable standard of reference, is a measure of pressure and reflects the functional consequence of narrowing in epicardial coronary vessels. The MBF index is a measure of flow, depends on epicardial coronary disease as well as myocardial microvascular dysfunction, and may be impaired in the absence of flow-limiting coronary artery narrowing but as a consequence of microvascular dysfunction. However, in our study, the presence of significant microvascular dysfunction was largely avoided by exclusion of patients with severely impaired left ventricular ejection fraction. Not all vessels were interrogated with FFR. The FFR was not performed in angiographically normal vessels, in vessels with <30% diameter narrowing or ≥90% diameter narrowing, in agreement with generally accepted clinical standards. Combining CTCA with CT perfusion imaging will increase patient radiation exposure. This could be justified provided that this approach decreases the false positive ratio of CTCA and hence the number of unnecessary invasive procedures. Technical developments such as more sophisticated detector arrays and iterative reconstruction algorithms may decrease radiation exposure in the near future. In addition, the combined approach requires a double dose of contrast agent, which necessitates careful selection of patients without impaired renal function. For these reasons, we did not test the reproducibility of the MBF index measurements on repeat scans.

Conclusions

In this proof-of-principle study, the CT evaluation of coronary artery anatomy and hyperaemic MBF index performed well as an integrated diagnostic tool to detect functionally significant coronary lesions in patients with stable angina, particularly in patients with intermediate coronary lesions. Future comparative effectiveness studies are warranted to assess the performance of such combined anatomical–physiological approach in a single non-invasive test in less-selected patient populations.

Funding

This work forms part of the research areas contributing to the translational research portfolio of the Cardiovascular Biomedical Research Unit at Barts, which is supported and funded by the National Institute for Health Research (NIHR). This study was partly supported by a grant from the FP7-CP-FP 2007 project (grant agreement 222915, EVINCI).

Conflict of interest: none declared.

Appendix 1 Patient preparation and scan protocol

Patient preparation

Patients abstained from caffeine (coffee, tea, chocolate, energy drinks etc.) for 18 h and from methylxanthine-containing products, theophylline, oral dipyridamole, beta-blockers, and nitrates for 24 h before the scan;
18-gauge cannula in the right antecubital vein for contrast injection; 20-gauge cannula in the left antecubital vein for adenosine infusion;
30-s breath hold practiced; if unable to hold the breath for longer than 20 s, patients were asked to exhale gently over 10 s.

Non-enhanced coronary calcium scoring

Collimation 2 × 32 × 1.2 mm;
Gantry rotation time 285 ms;
Voltage 120 kV;
Tube current–time product 75 mAs;
Slice thickness 3 mm, reconstruction increment 1.5 mm;
Image acquisition triggered 250 ms after the R-wave.

CTCA

Prospectively electrocardiogram (ECG)-triggered protocol (Adaptive Sequential, Siemens Healthcare);
Collimation 2 × 64 × 0.6 mm with z-flying focal spot (2 × 128 sections);
Gantry rotation time 285 ms;
Voltage/tube current–time product 100 kV/370 mAs if body mass index (BMI) <30; 120 kV/320 mAs if BMI >30;
Image acquisition triggered at 60–75% of R–R interval in heart rates of <65 bpm; 35–75% of R–R interval in heart rates between 65 and 80 bpm; 35–50% of R–R interval in heart rates >80 bpm.
Test bolus scan obtained with 6 s delay at the level of the ascending aorta after injection of 15 mL of contrast (Omnipaque 300, GE Healthcare or Ultravist 370, Schering, Berlin), followed by 40 mL of saline;
Main bolus of 50 or 60 mL of contrast (depending on the type used); Injection rates adjusted to achieve an iodine delivery rate of 2.2 g of iodine/s;
CTCA images reconstructed with 0.75 mm slice thickness and 0.4 mm increment using a medium-smooth convolution kernel (B26f).

10–15 min delay

CTP

Adenosine infused intravenously at a dose of 140 μg/kg/min and CTP acquisition started 3 min into the adenosine infusion;
ECG-triggered axial shuttle mode used (the scanner alternates rapidly between two table positions and acquires prospectively ECG-triggered axial images in these two positions over 30 s);
Collimation 2 × 32 × 1.2 mm;
Gantry rotation time 285 ms;
Voltage 100 kV;
Tube current–time product 300 mAs;
Image acquisition triggered 250 ms after the R-wave;
Scan delay calculated from the test bolus time-attenuation curve and set 6 s before arrival of contrast in the aorta;
50 or 60 mL of contrast injected with an iodine delivery rate of 2.2 g of iodine/s followed by 40 mL of saline;
Stress CTP images reconstructed with 3 mm slice thickness and 2 mm increment using a smooth-medium kernel that includes correction for iodine beam hardening (B23f).

Appendix 2 Flow-chart of CT image analysis

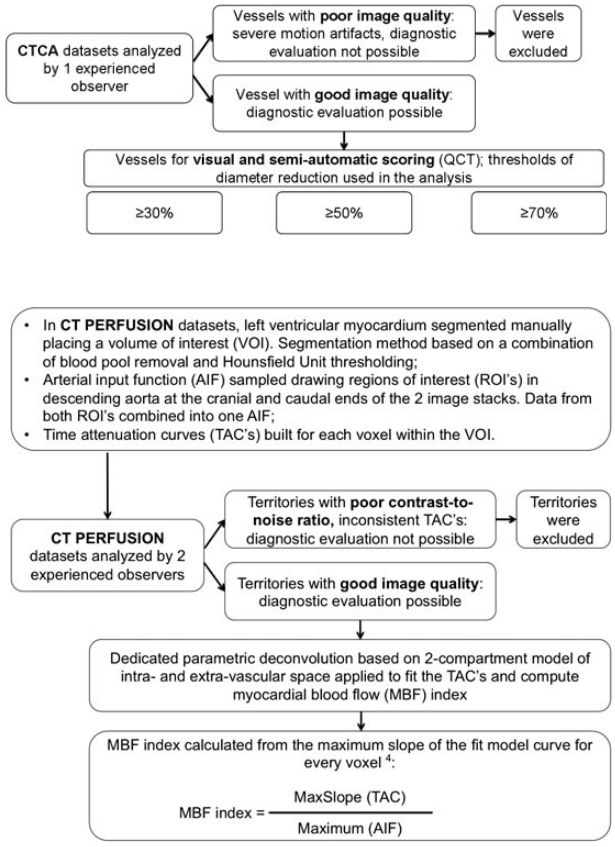

References

1. De Bruyne B, Pijls NH, Kalesan B, Barbato E, Tonino PA, Piroth Z *et al.* Fractional flow reserve-guided PCI versus medical therapy in stable coronary disease. *N Engl J Med* 2012;**367**:991–1001.
2. Bamberg F, Hinkel R, Schwarz F, Sandner TA, Baloch E, Marcus R *et al.* Accuracy of dynamic computed tomography adenosine stress myocardial perfusion imaging in estimating myocardial blood flow at various degrees of coronary artery stenosis using a porcine animal model. *Invest Radiol* 2012;**47**:71–7.
3. George RT, Jerosch-Herold M, Silva C, Kitagawa K, Bluemke DA, Lima JA *et al.* Quantification of myocardial perfusion using dynamic 64-detector computed tomography. *Invest Radiol* 2007;**42**:815–22.
4. Mahnken AH, Klotz E, Pietsch H, Schmidt B, Allmendinger T, Haberland U *et al.* Quantitative whole heart stress perfusion CT imaging as noninvasive assessment of hemodynamics in coronary artery stenosis: preliminary animal experience. *Invest Radiol* 2010;**45**:298–305.
5. Rossi A, Uitterdijk A, Dijkshoorn M, Klotz E, Dharampal A, van Straten M *et al.* Quantification of myocardial blood flow by adenosine-stress CT perfusion imaging in pigs during various degrees of stenosis correlates well with coronary artery blood flow and fractional flow reserve. *Eur Heart J Cardiovasc Imaging* 2012;**14**:331–8.
6. So A, Hsieh J, Li JY, Hadway J, Kong HF, Lee TY. Quantitative myocardial perfusion measurement using CT perfusion: a validation study in a porcine model of reperfused acute myocardial infarction. *Int J Cardiovasc Imaging* 2012;**28**:1237–48.
7. Bamberg F, Becker A, Schwarz F, Marcus RP, Greif M, von Ziegler F *et al.* Detection of hemodynamically significant coronary artery stenosis: incremental diagnostic value of dynamic CT-based myocardial perfusion imaging. *Radiology* 2011;**260**:689–98.
8. Ho KT, Chua KC, Klotz E, Panknin C. Stress and rest dynamic myocardial perfusion imaging by evaluation of complete time-attenuation curves with dual-source CT. *JACC Cardiovasc Imaging* 2010;**3**:811–20.
9. Wang Y, Qin L, Shi X, Zeng Y, Jing H, Schoepf UJ *et al.* Adenosine-stress dynamic myocardial perfusion imaging with second-generation dual-source CT: comparison with conventional catheter coronary angiography and SPECT nuclear myocardial perfusion imaging. *AJR Am J Roentgenol* 2012;**198**:521–9.

10. So A, Wisenberg G, Islam A, Amann J, Romano W, Brown J *et al.* Non-invasive assessment of functionally relevant coronary artery stenoses with quantitative CT perfusion: preliminary clinical experiences. *Eur Radiol* 2012;**22**:39–50.
11. Boogers MJ, Schuijf JD, Kitslaar PH, van Werkhoven JM, de Graaf FR, Boersma E *et al.* Automated quantification of stenosis severity on 64-slice CT: a comparison with quantitative coronary angiography. *JACC Cardiovasc Imaging* 2010;**3**:699–709.
12. Cerqueira MD, Weissman NJ, Dilsizian V, Jacobs AK, Kaul S, Laskey WK *et al.* Standardized myocardial segmentation and nomenclature for tomographic imaging of the heart: a statement for healthcare professionals from the Cardiac Imaging Committee of the Council on Clinical Cardiology of the American Heart Association. *Circulation* 2002;**105**:539–42.
13. Tonino PA, Fearon WF, De Bruyne B, Oldroyd KG, Leesar MA, Ver Lee PN *et al.* Angiographic versus functional severity of coronary artery stenoses in the FAME study fractional flow reserve versus angiography in multivessel evaluation. *J Am Coll Cardiol* 2010;**55**:2816–21.
14. Bossuyt PM, Reitsma JB, Bruns DE, Gatsonis CA, Glasziou PP, Irwig LM *et al.* Towards complete and accurate reporting of studies of diagnostic accuracy: the STARD initiative. *BMJ* 2003;**326**:41–4.
15. Genders TS, Spronk S, Stijnen T, Steyerberg EW, Lesaffre E, Hunink MG. Methods for calculating sensitivity and specificity of clustered data: a tutorial. *Radiology* 2012;**265**:910–6.
16. Blankstein R, Shturman LD, Rogers IS, Rocha-Filho JA, Okada DR, Sarwar A *et al.* Adenosine-induced stress myocardial perfusion imaging using dual-source cardiac computed tomography. *J Am Coll Cardiol* 2009;**54**:1072–84.
17. Feuchtner G, Goetti R, Plass A, Wieser M, Scheffel H, Wyss C *et al.* Adenosine stress high-pitch 128-slice dual-source myocardial computed tomography perfusion for imaging of reversible myocardial ischemia: comparison with magnetic resonance imaging. *Circ Cardiovasc Imaging* 2011;**4**:540–9.
18. George RT, Arbab-Zadeh A, Miller JM, Vavere AL, Bengel FM, Lardo AC *et al.* Computed tomography myocardial perfusion imaging with 320-row detector computed tomography accurately detects myocardial ischemia in patients with obstructive coronary artery disease. *Circ Cardiovasc Imaging* 2012;**5**:333–40.
19. Ko BS, Cameron JD, Meredith IT, Leung M, Antonis PR, Nasis A *et al.* Computed tomography stress myocardial perfusion imaging in patients considered for revascularization: a comparison with fractional flow reserve. *Eur Heart J* 2012;**33**:67–77.
20. Rocha-Filho JA, Blankstein R, Shturman LD, Bezerra HG, Okada DR, Rogers IS *et al.* Incremental value of adenosine-induced stress myocardial perfusion imaging with dual-source CT at cardiac CT angiography. *Radiology* 2010;**254**:410–9.
21. Techasith T, Cury RC. Stress myocardial CT perfusion: an update and future perspective. *JACC Cardiovasc Imaging* 2011;**4**:905–16.
22. Hajjiri MM, Leavitt MB, Zheng H, Spooner AE, Fischman AJ, Gewirtz H. Comparison of positron emission tomography measurement of adenosine-stimulated absolute myocardial blood flow versus relative myocardial tracer content for physiological assessment of coronary artery stenosis severity and location. *JACC Cardiovasc Imaging* 2009;**2**:751–8.
23. Kajander SA, Joutsiniemi E, Saraste M, Pietila M, Ukkonen H, Saraste A *et al.* Clinical value of absolute quantification of myocardial perfusion with (15)O-water in coronary artery disease. *Circ Cardiovasc Imaging* 2011;**4**:678–84.
24. Pijls NH, Sels JW. Functional measurement of coronary stenosis. *J Am Coll Cardiol* 2012;**59**:1045–57.
25. Chareonthaitawee P, Kaufmann PA, Rimoldi O, Camici PG. Heterogeneity of resting and hyperemic myocardial blood flow in healthy humans. *Cardiovasc Res* 2001;**50**:151–61.
26. Morton G, Chiribiri A, Ishida M, Hussain ST, Schuster A, Indermuehle A *et al.* Quantification of absolute myocardial perfusion in patients with coronary artery disease: comparison between cardiovascular magnetic resonance and positron emission tomography. *J Am Coll Cardiol* 2012;**60**:1546–55.
27. Mc Ardle BA, Dowsley TF, de Kemp RA, Wells GA, Beanlands RS. Does rubidium-82 PET have superior accuracy to SPECT perfusion imaging for the diagnosis of obstructive coronary disease?: A systematic review and meta-analysis. *J Am Coll Cardiol* 2012;**60**:1828–37.
28. Kajander S, Joutsiniemi E, Saraste M, Pietila M, Ukkonen H, Saraste A *et al.* Cardiac positron emission tomography/computed tomography imaging accurately detects anatomically and functionally significant coronary artery disease. *Circulation* 2010;**122**:603–13.
29. Meijboom WB, Van Mieghem CA, van Pelt N, Weustink A, Pugliese F, Mollet NR *et al.* Comprehensive assessment of coronary artery stenoses: computed tomography coronary angiography versus conventional coronary angiography and correlation with fractional flow reserve in patients with stable angina. *J Am Coll Cardiol* 2008;**52**:636–43.
30. Sarno G, Decraemer I, Vanhoenacker PK, De Bruyne B, Hamilos M, Cuisset T *et al.* On the inappropriateness of noninvasive multidetector computed tomography coronary angiography to trigger coronary revascularization: a comparison with invasive angiography. *JACC Cardiovasc Interv* 2009;**2**:550–7.
31. Wijns W, Kolh P, Danchin N, Di Mario C, Falk V, Folliguet T *et al.* Guidelines on myocardial revascularization. *Eur Heart J* 2010;**31**:2501–55.
32. Min JK, Leipsic J, Pencina MJ, Berman DS, Koo BK, van Mieghem C *et al.* Diagnostic accuracy of fractional flow reserve from anatomic CT angiography. *JAMA* 2012;**308**:1237–45.